Spectrochimica Acta, Vol. 36A, pp. 975 to 987

0584-8539/80/1101-0975$02.00/0

The i.r., Raman and microwave spectra of 1-butene-3-yne (vinylacetylene) and 1-butene-3-yne-4*d*

E. TØRNENG, C. J. NIELSEN and P. KLAEBOE
Department of Chemistry, University of Oslo, Oslo 3, Norway

and

H. HOPF and H. PRIEBE
Institute of Organic Chemistry, The Technical University of Braunschweig, D-3300, Braunschweig, West Germany

(*Received* 16 *April* 1980)

Abstract—The i.r. spectra of 1-butene-3-yne and 1-butene-3-yne-4*d* in the vapour phase and as crystalline solids at 90 K were recorded in the region 5000–100 cm^{-1}. Raman spectra, including semiquantitative polarization data, of the neat liquid and of the solid were obtained at 90 K. Microwave spectra of the compounds were recorded in the region 8–40 GHz at ambient temperature. Rotational transitions of the vibrational ground state and of the two lowest vibrational excited states $\nu_{13}(a')$ and $\nu_{18}(a'')$ were measured.

The fundamental frequencies of both compounds were assigned in excellent agreement with the results of normal coordinate calculations. Rotational fine structure was observed for several bands and interpreted as the *Q*-sub-branches of the perpendicular bands (in the symmetrical top approximation). For six bands the *Q*-sub-branches were assigned to the proper *K*-values. The Coriolis coupling constant $\xi^a_{13,18}$ was derived from the i.r. and from the microwave spectra.

INTRODUCTION

The vibrational spectra of 1-butene-3-yne (later to be called vinylacetylene, VA) were studied by several authors, the earlier work is referred to by KOHLRAUSCH [1] and SHEPPARD [2] who made tentative assignments. More recently, new i.r. and Raman spectra [3], photoelectron [4] and microwave [5–7] data were reported. The molecular structure in the vapour phase has been determined by electron diffraction [8]. Since no results are reported for 1-butene-3-yne-4*d* (4-deuterovinylacetylene VA-*d*) we wanted to make a thorough new study of the vibrational spectra of this molecule. With moderate resolution (*ca.* 0.5 cm^{-1}) well resolved rotational fine structure was observed for the perpendicular bands, making assignments according to the *K* quantum number feasible.

Extensive force field calculations were made on the two molecules combining vibrational and rotational spectroscopic data. The derived force field served as a basis for similar calculations on divinylacetylene and perchlorodivinylacetylene [9] which will be reported elsewhere.

In order to obtain accurate values for the *A* rotational constant, new microwave spectra of the parent and the deuterated molecule were recorded. Spectra of the first excited state of the two lowest fundamentals ν_{13} and ν_{18} were also recorded, revealing Coriolis coupling.

EXPERIMENTAL

Preparations. The undeuterated vinylacetylene is prepared by adding 130 ml of 1,4-dichloro-2-butene within 1 h to a solution of 400 g potassium hydroxide in 500 ml glycol and 100 ml of *n*-butyl-cellusolve (glykol-*n*-butyl ether) at 170°C. The enyne is condensed in a trap cooled with methanol/dry ice. Further purification is achieved by trap-to-trap distillation, and finally 14 ml of pure vinylacetylene is introduced into a boiling solution of 0.25 mol of ethylmagnesiumbromide in tetrahydrofuran. An efficient reflux condenser is connected to the reaction flask and cooled to −40°C during this grignardisation step to prevent the volatile enyne from escaping. After the reaction mixture has been cooled to room temperature 0.25 mol of D_2O is added dropwise. The crude 4-deuterovinylacetylene escapes from the reaction flask and is again trapped in a methanol-dry ice trap. Recondensation provides about 10 ml of pure 4-deuteriovinylacetylene (purity in excess of 98% as checked by GC-analysis on an OPN-column).

Microwave. The microwave spectra were recorded in the region 8–40 GHz at ambient temperature and at pressures less than 10 μm on a Hewlett–Packard 8460A MRR spectrometer. Stark voltages up to 1900 V/cm were applied and the measured frequencies are believed to be accurate within 0.05 MHz.

Infrared and Raman. The i.r. spectra were recorded on a Perkin–Elmer model 225 spectrometer (5000–200 cm^{-1}) and on a Bruker model 114 C fast scan evacuable Fourier transform spectrometer (4000–10 cm^{-1}). Vapour cells of path lengths 10 and 20 cm with windows of CsI and polyethylene, respectively, were employed. Cryostats, cooled with liquid nitrogen having windows of CsI and polyethylene were used, the samples were shock-frozen on the window and the spectra recorded before and after annealing.

Raman spectra were obtained on a Cary 81 spectrometer, modified for 90° illumination, excited by a CRL 52G argon ion laser. Spectra of the liquids at ambient temperature in sealed ampoules under pressure were recorded and semiquantitative polarization data obtained. The samples were deposited on a cooled copper block and the spectra recorded before and after annealing.

RESULTS

Microwave spectra

The microwave spectrum of VA has previously been investigated by several authors [5–7]. The dipole moments have been determined [5] to be: $\mu_a = 0.2$, $\mu_b \approx 0.02$ D.

The reported frequencies were either insufficient or too inaccurately measured to allow determination of the A rotational constant and the centrifugal distortion constants. In this investigation, only the $J = 3 \rightarrow 4$ transitions for the parent molecule were measured while the whole spectrum was remeasured for the 4d species. Transitions corresponding to the two lowest vibrational excited states, $\nu_{13}(a')$ and $\nu_{18}(a'')$ were also measured.*

In Table 1 the derived rotational parameters are given. As seen, there are large changes in the rotational constants for the $v_{13} = 1$ and $v_{18} = 1$ states due to Coriolis coupling of a- and b-type. However, the energy difference between the coupling states ($\nu_{13} = 217\ \text{cm}^{-1}$, $\nu_{18} = 305\ \text{cm}^{-1}$ for the parent molecule) is sufficiently large compared with A, so that no deviation from the semi-rigid rotor pattern was observed. The derivation of the Coriolis coupling constants will be discussed later in this paper.

Vibrational spectra

The i.r. spectra of VA and VA-d in the vapour phase are shown in Figs. 1 and 2, respectively. Raman spectra of the liquids are given in Fig. 3 (VA) and Fig. 4 (VA-d) whereas the solid state Raman spectrum of VA is shown in Fig. 5. The wave numbers of the observed i.r. and Raman bands are collected in Tables 2 (VA) and 3 (VA-d). The asssigned fundamentals for both molecules are listed in Table 8 together with the corresponding calculated frequencies.

From Table 1 it is seen that VA and VA-d are nearly symmetrical prolate rotors. With C_s symmetry, the 13 a' fundamentals will have A/B hybrid vapour contours, while the a'' modes can be distinguished by their C-type contours with prominent Q-branches. The PR separations for VA are *ca.* 18, 15 and 27 cm^{-1} for the A, B and C bands, respectively [10]. The well resolved (1) i.r. vapour contours, (2) Raman polarization measurements, (3) the additional spectra of VA-d and finally (4) the force constant calculations, make the assignments for VA and VA-d quite unambiguous.

Thus, in VA the i.r. vapour bands at 974, 927, 676, 618 and 305 cm^{-1} with sharp Q-branches, all of which except the 618 cm^{-1} band had depolarized Raman counterparts, are obviously the five a'' modes $\nu_{14} - \nu_{18}$. Among the four C—H stretches ($\nu_1 - \nu_4$), the assignments are definite except for ν_3. We have assigned this mode to the weak vapour band at 3068 cm^{-1}, of which only the high frequency branch at 3075 cm^{-1} is visible, appearing around 3050 cm^{-1} in the liquid and crystalline states.

The remaining a' fundamentals were assigned to strong or medium intense (although the 1096 cm^{-1} band was only weak) polarized Raman bands. The i.r. counterparts varied from very weak (ν_5 and ν_8) to very strong (ν_{11}). In every case the band contours appeared as pure B or as A/B hybrids with PR separations close to the predicted values.

The i.r. and Raman spectra of VA-d were practically identical to those of VA concerning band intensities and contours. Except the ≡C—H stretching and bending modes which obviously are highly displaced on deuteration and some skeletal modes like ν_5, ν_{10}, ν_{13} and ν_{18} which are displaced less than 20 cm^{-1}, the bands of VA and VA-d are coinciding.

The a'' modes ν_{14}–ν_{18} of VA-d are easily assigned to the appropriate C-type i.r. vapour bands. Here, the in-plane and out-of-plane C≡C—D

* The microwave spectra of the two molecules are available from the authors upon request, or from the Microwave Data Center, Molecular Spectroscopy Section, National Bureau of Standards, Washington, DC 20234, U.S.A., where they have been deposited.

Table 1. Rotational constants for the ground, the $v_{13} = 1$ and the $v_{18} = 1$ states of 1-butene-3-yne and 1-butene-3-yne-4d. Rotational constants (A, B, C) and S.D. of fit (σ) in MHz. Distortion constants (D_J, D_{JK}) in kHz. Inertial defect (ID) in uÅ^2. Numbers in parantheses represent 1 S.D.

	1-butene-3-yne						1-butene-3-yne-4d					
	ground state		$v_{13} = 1$		$v_{18} = 1$		ground state		$v_{13} = 1$		$v_{18} = 1$	
A	50308.	(55)	49274.	(59)	51676.	(53)	49393.	(34)	48337.	(36)	50866.	(49)
B	4744.9317	(77)	4763.276	(11)	4747.7146	(81)	4403.9538	(40)	4420.6331	(43)	4406.1168	(51)
C	4329.7899	(77)	4337.5385	(99)	4338.6433	(83)	4037.8007	(40)	4044.8607	(43)	4045.6294	(51)
D_J	1.93	(22)	2.17	(28)	1.86	(21)	1.56	(11)	1.60	(12)	1.60	(14)
D_{JK}	-83.22	(67)	-70.90	(86)	-93.19	(64)	-77.35	(34)	-66.43	(46)	-88.66	(44)
ID	0.167	(11)	0.157	(12)	0.257	(10)	0.1744	(72)	0.1653	(77)	0.2848	(96)
σ	0.0419		0.0495		0.0365		0.0214		0.0235		0.0274	

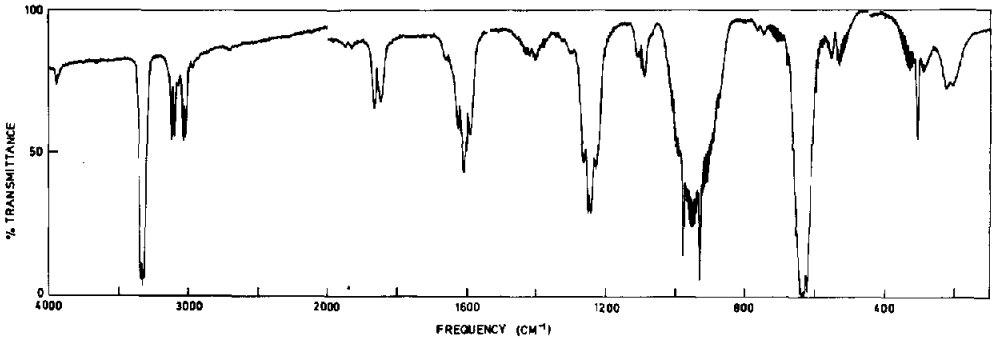

Fig. 1. Infrared vapour spectrum of 1-butene-3-yne (VA).

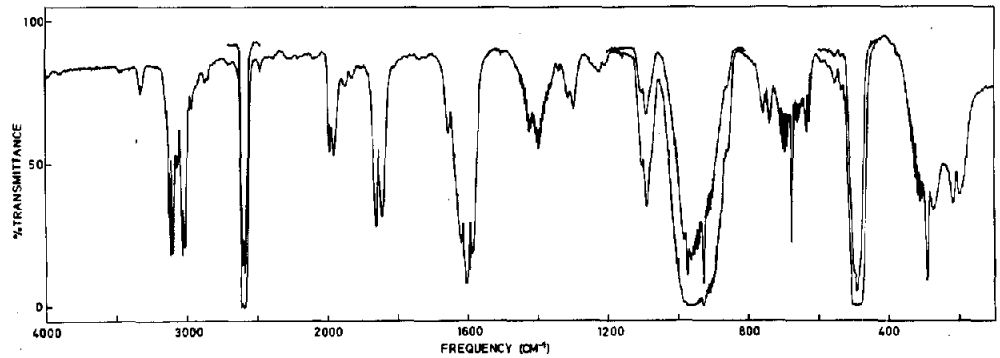

Fig. 2. Infrared vapour spectrum of 1-butene-3-yne-4*d* (VA-*d*).

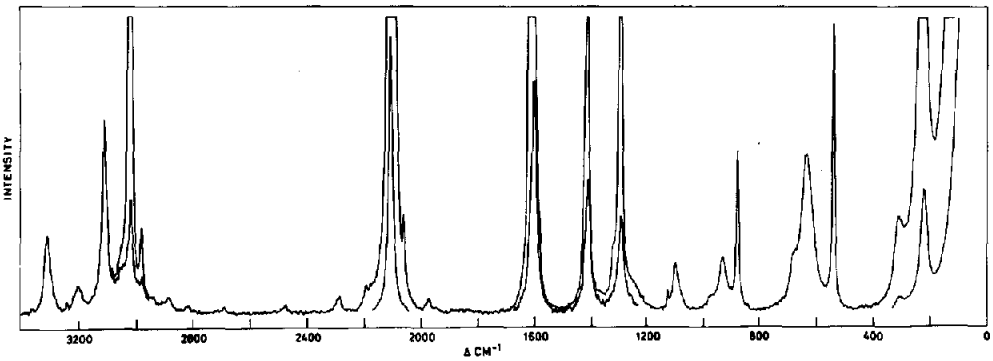

Fig. 3. Raman spectrum of liquid 1-butene-3-yne (VA)

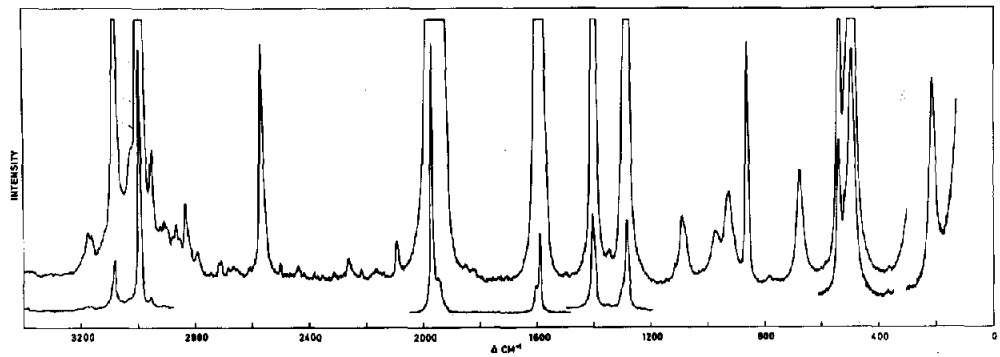

Fig. 4. Raman spectrum of liquid 1-butene-3-yne-4*d* (VA-*d*)

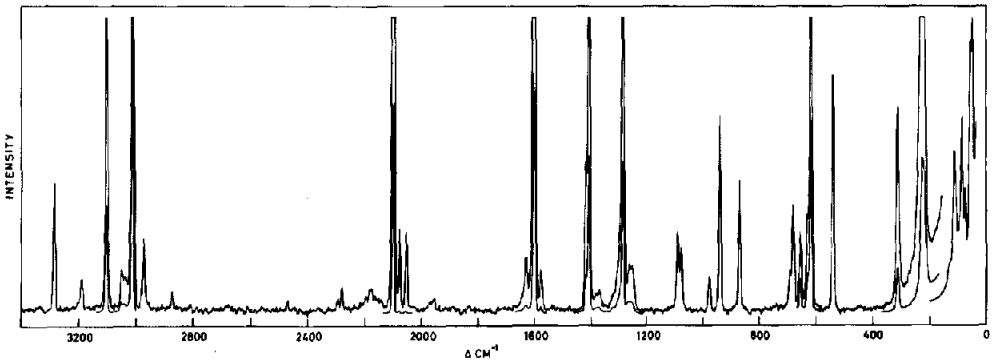

Fig. 5. Raman spectrum of 1-butene-3-yne (VA) as a crystalline solid at *ca.* 90 K.

Table 2. Infrared and Raman spectral data* for 1-butene-3-yne (vinylacetylene)

Infrared		Raman		Interpretation
Vapour	Cryst(-180°C)	Liquid	Cryst(-180°C)	
3342 vs+				
3330 vs	3287 vs	3300 m,P	3287 m	ν_1 a'
3347 vs				
3126 m				
3114 m A/B	3106 m	3105 m, P	3105 s	ν_2 a'
3105 m				
3075 w B?	3050 vw	3048 vw, D?, sh	3052 w, 3037 w	ν_3 a'
3046 m				
3030 m A/B	3015 m	3015 s, P	3015 vs	ν_4 a'
3023 m				
2990 w B?	2973 vw	2974 w, P	2974	$\nu_6 + \nu_7$ = 3014 A'
2985 w				
	2958 vw			$\nu_5 + \nu_{15}$ = 3037 A"
	2919 vw			$\nu_5 + \nu_{10}$ = 2984 A'
	2875 vw	2876 vw, P	2875 vw	$\nu_6 + \nu_8$ = 2910 A'
2740 vw B?	2755 vw			$\nu_5 + \nu_{16}$ = 2786 A"
2720 vw				
2704 vw B?		2685 vw, P?	2688 vw	$\nu_6 + \nu_9$ = 2695
2698 vw			2677 vw	
2656 vw B?	2640 vw			$\nu_5 + \nu_{12}$ = 2650 A'
2636 vw				
		2471 vw, P	2469 vw	$\nu_7 + \nu_9$ = 2511 A'
		2291 w, P	2293 vw	$\nu_5 + \nu_{13}$ = 2325 A'
2305 vw				
2292 vw C?	2280 vw	2282 w, P	2279 w	$\nu_7 + \nu_{10}$ = 2289 A'
2277 vw				
			2203 vw	$\nu_8 + \nu_{15}$ = 2238 A"
			2193 vw	$\nu_6 + \nu_{17}$ = 2217 A"
		2187 w, P	2177 w	$\nu_6 + \nu_{11}$ = 2229 A'
			2162 w	$2\nu_9$ = 2192 A'
			2142 w	$\nu_8 + \nu_{10}$ = 2185 A'
2117 vw A/B?	2101 w	2102 vs, P	2099 vs	ν_5 a'
2105 vw				
			2078 w	$\nu_7 + \nu_{16}$ = 2091 A"
		2056 m, D?	2052 w	$\nu_9 + \nu_{14}$ = 2070 A"
1975 vw, B?	1954 m	1969 w, P		$\nu_9 + \nu_{10}$ = 1970 A'

Table 2. (*contd.*)

Infrared		Raman		Interpretation
Vapour	Cryst(-180°C)	Liquid	Cryst(-180°C)	
1943 w, 1927 w } B?	1923 vw, 1918 vw }	1937 vw, P?		$2\nu_{14}$ = 1948 A'
	1918 vw			$\nu_7 + \nu_{12}$ = 1955 A'
		1870 vw, D?		$\nu_6 + \nu_{18}$ = 1904 A"
1868 m, 1856 m, 1848 m } A/B	1889 s	1827 vw, P?		$2\nu_{15}$ = 1854 A'
1757 vw, 1743 vw } B?				$2\nu_{10}$ = 1748 A'
1660 w, 1652 w, 1643 w } A/B	1665 m			$\nu_9 + \nu_{11}$ = 1726 A'
1626 m, 1616 m, 1609 m } A/B	1632 vw	1610 m, P?	1630 w	$\nu_{14} + \nu_{16}$ = 1650 A' FR
1609 m, 1599 m, 1591 m } A/B	1599 vs	1599 vs, P	1602 vs	ν_6 a'
	1576 vw	1579 w, sh, P	1578 w	$\nu_{14} + \nu_{17}$ = 1592 A'
	1421 m, 1419 m	1416 w, D?	1419 m	$\nu_{12} + \nu_{15}$ = 1467 A"
1420 w, 1403 w } B	1408 s, 1405 m, sh	1407 s, P	1408 s	ν_7 a'
1370 vw,	1370 m, br	1361 vw, P	1373 vw	$\nu_{10} + \nu_{12}$ = 1414 A'
1320 vw	1293 m	1289 s,p	1286 s	ν_8 a'
1305 vw, 1300 vw, 1282 vw }	1319 m	1316 vw, P		$\nu_9 + \nu_{12}$ = 1311 A'
1265 m, 1252 s, 1244 s } A/B	1266 m, sh, 1260 s, 1251 s }		1265 w, 1254 w }	$2\nu_{11}$ = 1260 A'
1244 s, 1230 m } B?	1240 vw, 1227 vw }	1240 vw, P?		$2\nu_{17}$ = 1236 A"
	1218 vw			$\nu_{11} + \nu_{17}$ = 1248 A"
1106 m, 1096 m, 1088 m } A/B	1094 m, 1082 m }	1096 w, P	1093 m	ν_9 a'
1065 vw	1075 vw, sh	1077 vw, D?		$\nu_{10} + \nu_{13}$ = 1089 A'
974 vs, C	980 vs	968 vw, sh, D	979 w	ν_{14} a"
927 vs, C	943 vs, 934 s, sh }	931 w, D	942 m	ν_{15} a"
	888 vw			$\nu_{17} + \nu_{18}$ = 923 A'
874 m, A/B	876 s	879 m, P	874 m	ν_{10} a'
	868 vw			$\nu_{11} + \nu_{13}$ = 862 A"
801 vw, 794 vw, 787 vw } A/B?	784 vw			$\nu_{12} + \nu_{18}$ = 843 A"
760 vw, 742 vw } B	769 w, 757 vw }			$\nu_{12} + \nu_{13}$ = 755 A'
676 w, C	693 s, 665 vs, 661 vw }	675 vw, sh, D	695 w, 684 m, 658 w }	ν_{16} a"

Table 2. (*contd.*)

Infrared		Raman		Interpretation
Vapour	Cryst(-180°C)	Liquid	Cryst(-180°C)	
634 vs, 625 vs } B?	636 m, sh	634 m, br, P?	634 m	ν_{11} a'
618 vs, C	628 vs		621 s	ν_{17} a"
550 m, 525 m } B	542 vs, 534 vw }	540 m, P	543 m	ν_{12} a'
		443 vw, P?		$2\nu_{13}$ = 448 A'
305 m, C	326 s, 311 s }	309 w, D	314 m	ν_{18} a"
226 m, 208 w } B	229 s	224 m, P	228 m, 221 m	ν_{13} a'
			132 w, 115 m, 89 m }	lattice modes

* Bands above 3400 cm^{-1} and weak bands outside the fundamental regions have been omitted.

† Abbreviations: s, strong; m, medium; w, weak; v, very; br, broad; sh, shoulder; P, polarized; D, depolarized; A, B and C denote band contours.

Table 3. Infrared and Raman spectral data for 1-butene-3-yne-4*d* (vinylacetylene-4*d*)

Infrared		Raman	Interpretation
Vapour	Cryst (-180°C)	Liquid	
3340 w, 3329 w, 3319 w } A/B	3286 m		Parent
3123 s, 3114 s, 3106 s } A/B	3105 m	3099 m, P	ν_1 a'
	3070 w		$\nu_4 + \nu_{17}$ = 3095 A"
3075 m } B	3054 w, 3048 vw, sh }	3054 w	ν_2 a'
3038 s, 3031 s, 3022 s } A/B	3014 m	3019 vs, P	ν_3 a'
2984 w, 2972 w } B	2972	2978 m, P	$\nu_7 + \nu_6$ = 3010 A'
	2955 vw, br	2948 m, P	$\nu_5 + \nu_{14}$ = 2968 A"
	2922 vw, br	2929 w, D	$\nu_5 + \nu_{14}$ = 2968 A"
	2871 vw	2881 w, D	$\nu_6 + \nu_8$ = 2902 A'
2871 vw, 2863 vw, 2853 vw } A/B	2842 w	2856 vw, D	$\nu_4 + \nu_{18}$ = 2896 A"
		2818 w, P	$2\nu_7$ = 2830 A'
		2691 vw, P	$\nu_6 + \nu_9$ = 2692 A'
2616 vs, 2605 vs, 2598 vs } A/B	2577 vs, 2570 m, sh, 2566 w }	2591 s, P	ν_4 a'

Table 3. (*contd.*)

Infrared		Raman	Interpretation
Vapour	Cryst (−180°C)	Liquid	
2002 m			
1995 m	1978 vs, sh	1984 vs, P	ν_5 a'
1993 m	1977 vs		
1984 m			
	1969 vw	1964 m, P	$\nu_8 + \nu_{16}$ = 1982 A"
1948 vw, 1930 vw } B	1960 m, 1953 m }		$2\nu_{14}$ = 1948 A"
	1891 m, sh		
	1887 s		$\nu_{14} + \nu_{15}$ = 1901 A"
	1880 m, sh		
1863 m, 1855 m, 1845 m } A/B		1839 vw, D	$2\nu_{15}$ = 1854 A"
1657 w, 1649 w } A/B	1664 m, 1662 m, 1652 vw, sh }	1657 vw, sh, D	$\nu_{14} + \nu_{16}$ = 1650 A"
1619 s, 1613 s, 1604 s } A/B	1630 w	1613 m, P	$\nu_9 + \nu_{11}$ = 1639 A'
1604 s, 1596 s, 1588 s } A/B	1597 s	1600 vs, P	ν_6 a'
	1575 w	1580 m, P	$\nu_9 + \nu_{12}$ = 1586 A'
1426 w, 1399 m } B	1413 s, 1410 m, sh, 1404 s }	1414 vs, P	ν_7 a'
1364 vvw, 1338 vvw } B	1365 m	1360 w, P	$2\nu_{16}$ = 1352 A"
1314 w, 1306 w, 1296 w } A/B	1291 w	1291 vs, P	ν_8 a'
1298 vw, C			
1103 m, 1100 m, 1095 m, 1089 m } A/B	1096 m	1097 m, P	ν_9 a'
1089 m, 1075 m } B	1083 m	1087 m, P	$2\nu_{11}$ = 1086 A'
	1054 m		$\nu_{13} + \nu_{10}$ = 1070 A'
	1015 m		$\nu_{11} + \nu_{12}$ = 1033 A'
974 vs, C	992 w, sh, 981 vs }	979 w, D	ν_{14} a"
927 vs, C	943 vs, 934 m }	935 m, D	ν_{15} a"
865 m, 858 m } A/B	865 m	869 s, P	ν_{10} a'

Table 3. (*contd.*)

Infrared		Raman	Interpretation
Vapour	Cryst (-180°C)	Liquid	
757 w, 749 w, 745 w } A/B	761 m		$\nu_{12} + \nu_{18}$ = 781 A"
			$\nu_{17} + \nu_{18}$ = 781 A'.
739 w			
	689 s		$\nu_{12} + \nu_{13}$ = 695 A'
	682 m		$\nu_{13} + \nu_{17}$ = 695 A"
676 m, C	661 m	682 s, D	ν_{16} a"
632 w, 624 w, 618 w	645 vw, 630 m, 612 vw		Parent
552 w, 534 w } B	545 m	544 vs	ν_{11} a'
500 vs, 490 vs, 482 vs	520 m, 506 m, 496 vs	499 vs, D	ν_{12} a', ν_{17} a"
		369 vw	
291 s, C	325 m, sh, 316 vs, 300 s	295 vw	ν_{18} a"
215 m, 195 m } B	220 s	217 s, P	ν_{13} a'

* Bands above 3400 cm^{-1} and weak bands outside the fundamental regions have been omitted.

† Abbreviations: s, strong; m, medium; w, weak; v, very; br, broad; sh, shoulder; P, polarized; D, depolarized; A, B and C denote band contours.

bending apparently coincide around 490 cm^{-1} while for VA they appeared as barely separated bands at 625 (a') and 618 cm^{-1} (a'').

The three vinylic C—H stretching modes in VA-*d* fall at the same wave numbers as in VA, whereas the acetylenic C—D is situated at 2605 cm^{-1}. The a' fundamentals ν_5, ν_6, ν_7, ν_9 and ν_{10} all had the expected frequency shift from VA to VA-*d* and were assigned with certainty. In VA-*d* ν_8 appeared as a well resolved vapour band with *A*/*B* hybrid contour at 1306 cm^{-1}, having a very strong Raman counterpart at 1291 cm^{-1}. The spectra of VA are more complex in this region since various combination bands involving ν_{11} and ν_{17} (C≡C—H deformation) appear in this region. Tentatively, the *A*/*B* hybrid contour with centre at 1312 cm^{-1} corresponding to the Raman band at 1289 cm^{-1} was attributed as ν_8 in VA. The bands around 1291 cm^{-1} in the vapour apparently correspond to 1319 in the crystal spectrum and were assigned as $\nu_9 + \nu_{13}$ (A') since the vapour-crystal shift for ν_{13} is significant.

In VA-*d* ν_{12} (overlapping ν_{17}) appears with high intensity at 490 cm^{-1} and pushes ν_{11} to 543 cm^{-1} at slightly higher wave number than the value at 540 cm^{-1} in VA. Finally, the lowest a' mode ν_{13} appears as a *B*-band at 205 cm^{-1} with a strong, polarized counterpart in Raman at 217 cm^{-1}.

The bands not considered as fundamentals can all be well explained as overtones or combination bands. In the spectra of VA-*d* a very small impurity of the parent molecule appeared as weak bands at 3330, 625 and 618 cm^{-1}.

ROTATIONAL FINE STRUCTURE AND CORIOLIS COUPLING

The i.r. vapour bands showed well resolved rotational fine structure for the perpendicular type bands where the *Q*-branch splitting is *ca.* 3 cm^{-1}. The splitting of the *P*- and *R*-branches in the parallel type bands, calculated to be *ca.* 0.3 cm^{-1}, could not be resolved with our present instrumentation.

Various perpendicular type fundamentals (in the symmetric top approximation) had resolved rotational band structure which could be assigned to the proper K-values. In VA ν_2, ν_{12} and ν_{13} of species a' and ν_{16} and ν_{18} of species a'' were employed for these calculations, the best resolution was provided by ν_{12} with a centre at 540 cm^{-1}. The fact that the C≡C—H bending modes were shifted from *ca.* 625 cm^{-1} in VA to 490 cm^{-1} in VA-*d* led to partly overlap with the 543 cm^{-1} band. Instead, ν_{16} at 676 cm^{-1} was better resolved in VA-*d* and so was ν_7 at 1414 cm^{-1}.

A calculation of the band shape and fine structure [11] revealed that the major contribution to the Q-branches in the perpendicular bands arise from transitions with J quantum number in the range 20–50 and that for $|K|>4$ the deviation from the symmetric rotor pattern is negligible. Hence, these sub-branches may within a good approximation be fitted to the expression:

$$\nu_{K''\to K'} = \nu_0 + (A''-\bar{B}'')\cdot K''^2 - (A'-\bar{B}') \cdot K'^2 - D''_K \cdot K''^4 + D'_K \cdot K'^4$$

where $\bar{B}$ equals $\frac{1}{2}(B+C)$.

The observed fine structure for all the fundamentals mentioned above were fitted simultaneously to this expression and the various parameters (ν_0, $A-\bar{B}$ and D_K) resulting from this procedure are collected in Table 4. For comparison, the values of $A-\bar{B}$ from the microwave investigation are also included in Table 4. As seen, the results from i.r. and microwave analyses agree within the experimental uncertainties.

As an example the absorption spectra from 180 to 370 cm^{-1} of VA, recorded at *ca.* 0.5 cm^{-1} resolutilon are given in Fig. 6. The lowest modes of each species $\nu_{13}(a')$ and $\nu_{18}(a'')$ are situated in this region. The observed wave numbers for each sub branch in VA and VA-*d* are listed in Table 5.

From the values of $A-\bar{B}$ in Table 4 it is seen that the $v_{13}=1$ and $v_{18}=1$ states are strongly perturbed, obviously these states are coupled by a Coriolis interaction. Following the method outlined by Mills [12], the Coriolis coupling constant $\xi^a_{13,18}$ was found from the rotational fine structure of the ν_{13} and ν_{18} bands. For VA, $\xi^a_{13,18}$ was found to be 0.58 ± 0.05 while the corresponding value for VA-*d* was 0.61 ± 0.05.

As mentioned before, the $v_{13}=1$ and $v_{18}=1$ states are coupled by both a- and b-type Coriolis interactions. Since we have accurate values for all rotational constants for these states from the microwave investigation it is possible to determine both $\xi^a_{13,18}$ and $\xi^b_{13,18}$. Neglecting interactions from all other vibrational states, the contribution to the effective rotational constants from the Coriolis interaction is given by

$$A^s_{(cor)} = \frac{G_a^2}{\Delta_{sr}} - \frac{(A-C)G_b^2}{\Delta_{sr}^2} + \frac{G_a^2 G_b^2}{\Delta_{sr}^2(A-B)},$$

$$B^s_{(cor)} = \frac{G_b^2}{\Delta_{sr}} - \frac{(B-C)G_a^2}{\Delta_{sr}^2} - \frac{G_a^2 G_b^2}{\Delta_{sr}^2(A-B)},$$

Table 4. Calculated band centres (ν_0)*, rotational constants ($A-\bar{B}$) and centrifugal distortion constants (D_K) obtained from i.r. and microwave spectra

	ν_0	$A-\bar{B}_{i.r.}$	$A-\bar{B}_{mw}$	D_K
		$H_2C{=}CH{-}C{\equiv}CH$		
ground state		1.5249 (16)	1.5268 (18)	8.3 (6)
v_2 = 1	3116.39(11)	1.5138 (23)		4.9 (11)
v_{12}= 1	539.21(3)	1.5189 (17)		8.3 (7)
v_{13}= 1	217.21(13)	1.487 (4)	1.4918 (20)	5.2 (22)
v_{16}= 1	677.40(23)	1.557 (6)		13. (3)
v_{18}= 1	303.56(7)	1.5742 (21)	1.5722 (18)	11.6 (8)
		$H_2C{=}CH{-}C{\equiv}CD$		
ground state		1.4975 (21)	1.5068 (11)	6.7 (7)
v_1 = 1	3114.22(9)	1.5003 (29)		9.7 (11)
v_7 = 1	1415.28(10)	1.495 (3)		2.0 (14)
v_{13}= 1	205.10(19)	1.463 (5)	1.4712 (12)	3.0 (28)
v_{15}= 1	926.49(9)	1.483 (3)		4.5 (10)
v_{16}= 1	675.99(9)	1.5114 (25)		8.1 (8)
v_{18}= 1	289.91(9)	1.5501 (27)	1.5558 (16)	11.3 (10)

* ν_0 and $A-\bar{B}$ in cm^{-1}, D_K in 10^{-5} cm^{-1}.

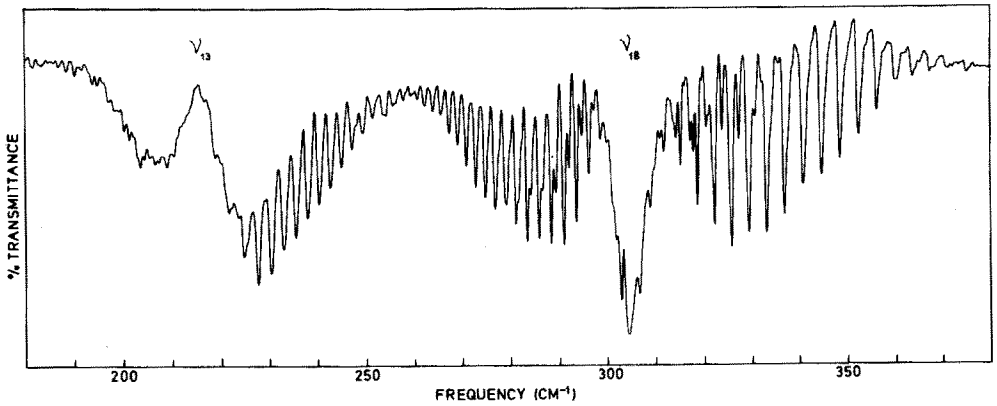

Fig. 6. Infrared spectrum of the ν_{13} and ν_{18} bands in 1-butene-3-yne (VA) at *ca.* 0.5 cm^{-1} resolution.

Table 5. The υ_{13} and υ_{18} bands (cm^{-1}) of 1-butene-3-yne and 1-butene-3-yne-4*d*

K-values in ^RQ_K ^PQ_K	$CH_2{=}CH{\equiv}CH$				$CH_2{=}CH{\equiv}CD$			
	υ_{18}		υ_{13}		υ_{18}		υ_{13}	
	Obs.	Obs.-calc.	Obs.	Obs.-calc.	Obs.	Obs.-calc.	Obs.	Obs.-calc.
15	359.90	-0.12			345.31	-0.10		
14	356.04	-0.12			341.57	-0.17		
13	352.18	-0.11			337.96	-0.04		
12	348.32	-0.08	249.12	0.04	334.22	-0.01	237.20	0.07
11	344.59	0.06	246.84	-0.06	330.49	0.05	234.79	-0.05
10	340.73	0.06	244.67	0.01	326.63	-0.02	232.50	-0.03
9	336.75	-0.09	242.38	0.00	322.89	0.02	230.09	-0.09
8	333.02	-0.03	239.97	-0.06	319.16	0.04	227.80	0.01
7	329.28	-0.03	237.68	0.06	315.42	0.01	225.38	0.02
6	325.54	-0.08	235.15	0.01	311.80	0.05	222.97	0.10
5	322.05	0.04	232.62	0.03	308.19	0.03	220.44	0.13
4	318.43	-0.03	229.96	-0.01	304.69	0.05		
3	315.06	0.06	227.31	0.04	301.32	0.11		
2	311.56	-0.06	224.42	-0.07				
3	295.89	-0.25						
4	293.36	0.02			279.86	-0.05		
5	290.71	0.07			277.33	0.05		
6	288.06	0.01			274.80	0.04		
7	285.65	0.09			272.27	-0.07		
8	283.24	0.08			269.86	-0.15		
9	280.83	-0.02			267.57	-0.20		
10	278.78	0.14			265.64	0.04		
11	276.61	0.10			263.47	-0.04		
12	274.56	0.10			261.42	-0.06		
13	272.51	0.03			259.49	0.00		
14	270.58	0.01			257.69	0.15		
15	268.65	-0.07			255.64	0.02		
16	266.97	0.06			253.95	0.25		
17	265.16	0.01						
18	263.47	0.06						
19	261.78	0.09						

where Δ_{sr} is the energy difference between the coupling states s and r. G_a and G_b are given by

$$G_a = A\xi^a_{sr}[(\nu_r/\nu_s)^{\frac{1}{2}} + (\nu_s/\nu_r)^{\frac{1}{2}}],$$
$$G_b = B\xi^b_{sr}[(\nu_r/\nu_s)^{\frac{1}{2}} + (\nu_s/\nu_r)^{\frac{1}{2}}].$$

Since ν_{13} corresponds to an in-plane mode, the effective rotational constants for this state further have a harmonic as well as an anharmonic contribution of unknown magnitude. This is not the case for the $\upsilon_{18}=1$ state (out-of-plane mode). Hence, we have not used the rotational constants for the $\upsilon_{13}=1$ state in determining the Coriolis coupling constants. For VA the derived constants were: $\xi^a_{13,18}=0.58\pm0.05$ and $\xi^b_{13,18}=0.28\pm0.05$. The corresponding values for VA-*d* were: $\xi^a_{13,18}=0.61\pm0.05$ and $\xi^b_{13,18}=0.26\pm0.05$.

FORCE CONSTANT CALCULATIONS

A non-redundant set of symmetry coordinates, based on the valence coordinates indicated on Fig. 7 is given in Table 6. The molecular geometry was taken as the r^0-structure [8] with a linear acetylene chain.

An initial valence force field was constructed on the basis of spectroscopic data on ethylene [14], monohalo ethylenes [15] and vinylidene halides [16]. Force constant calculations on the out-of-plane modes for the monohalo ethylenes indicate remarkably constant values for the interaction constants. Hence, we have transferred these interaction constants to VA. We have further transferred the values for the *cis* and *trans* C=C—H bending interaction constants found for ethylene.

The force field was then refined by the least squares method using the observed vibrational frequencies, the Coriolis coupling constants and the centrifugal distortion constants. The weights assigned to each value was taken as $1/\sigma_i^2$, where σ_i was estimated as 1% of the vibrational frequencies and 5% or 1 S.D., whichever is the largest, for the distortion constants. For the Coriolis coupling constants, σ_i was taken as two times the S.D. to allow for anharmonicity effects.

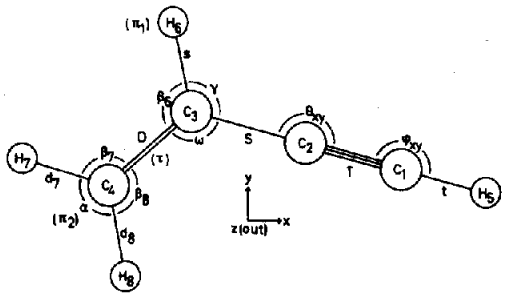

Fig. 7. Valence coordinates for 1-butene-3-yne. π_1 and π_2 denote out-of-plane bending coordinates involving atoms 4, 2, 3, 6 and 8, 7, 4, 3 while τ denotes torsion around the C=C bond.

Table 6. Internal valence symmetry coordinates for 1-butane-3-yne with reference to Fig. 7

$S_1(a')$	=	T
$S_2(a')$	=	D
$S_3(a')$	=	S
$S_4(a')$	=	t
$S_5(a')$	=	$2^{-\frac{1}{2}}(d_7 + d_8)$
$S_6(a')$	=	$2^{-\frac{1}{2}}(d_7 - d_8)$
$S_7(a')$	=	s
$S_8(a')$	=	θ_{xy}
$S_9(a')$	=	$6^{-\frac{1}{2}}(2\omega - \beta_6 - \gamma)$
$S_{10}(a')$	=	$2^{-\frac{1}{2}}(\beta_6 - \gamma)$
$S_{11}(a')$	=	$6^{-\frac{1}{2}}(2\alpha - \beta_7 - \beta_8)$
$S_{12}(a')$	=	$2^{-\frac{1}{2}}(\beta_7 - \beta_8)$
$S_{13}(a')$	=	ϕ_{xy}
$S_{14}(a'')$	=	ϕ_z
$S_{15}(a'')$	=	θ_z
$S_{16}(a'')$	=	$\frac{1}{2}(\tau_{8436} + \tau_{8432} + \tau_{7432} + \tau_{7436})$*
$S_{17}(a'')$	=	τ_{8743} (π_2)
$S_{18}(a'')$	=	τ_{4236} (π_1)

* τ_{ijkl} and π_{ijkl} denote torsion and out-of-plane bending coordinates involving atoms *i*, *j*, *k* and *l* as defined in Ref. [13].

Table 7. Derived valence force constants for 1-butene-3-yne

Constant	value*	Constant	value	
	stretch		stretch-stretch	
K_T	15.334 (28)†	F_{SD}	0.5	- §
K_S	5.252 (27)	F_{ST}	0.2	-
K_D	9.148 (28)	F_{dd}	0.039	(22)
K_t	5.976 (26)		stretch-bend	
K_s	5.111 (25)	$F_{D\beta}$, $F_{S\gamma}$	0.336	(15)
K_d	5.144 (22)	$F_{D\omega}$, $F_{S\omega}$	0.276	(25)
	bend		bend-bend	
H_β	0.5820(73)	$f^{trans}_{\beta\beta}$, $f^{trans}_{s\omega}$	0.067	-
H_α	0.3654(90)			
H_γ	0.572 (16)	$f^{cis}_{\beta\beta}$, $f^{cis}_{s\omega}$	-0.034	-
H_ω	0.842 (18)			
$H_{\theta_{xy}}$	0.2721(62)	$f_{\theta_{xy}\phi_{xy}}$	0.100	(10)
H_{θ_z}	0.3041(33)			
$H_{\phi_{xy}}$	0.2206(32)	$f_{\theta_z\phi_z}$	0.0735	(89)
H_{ϕ_z}	0.2057(38)	$f_{\Pi_1\Pi_2}$	0.04	-
H_τ	0.09744(14)	$f_{\Pi_1\tau_2}$	-0.035	-
H_{Π_1}	0.3823(46)			
H_{Π_2}	0.2383(27)			

* Units for stretching and stretch–stretch interaction constants are mdyn Å^{-1}, for bending constants units are mdyn · Å rad^{-2}, and stretch–bend interaction constants have units of mdyn rad^{-1}.

† Numbers in parentheses represent 1 S.D.

§ Constrained.

Table 8. Observed and calculated spectroscopic data for 1-butene-3-yne and 1-butene-3-yne-4*d*. Vibrational frequencies (ν_i) in cm^{-1}, centrifugal distortion constants (D_J, D_{JK}, D_K) in kHz and inertial defect (ID_c) in uÅ^2

	No	Observed	Calculated	PED*	Observed	Calculated	PED
			CH_2=CH-C≡CH			CH_2=CH-C≡CD	
a'	ν_1	3330	3344	96 S_4	3114	3115	98 S_6
	ν_2	3116	3115	98 S_6	3068	3068	93 S_7
	ν_3	3068	3068	93 S_7	3030	3030	94 S_5
	ν_4	3030	3030	94 S_5	2605	2594	28 S_1 + 70 S_4
	ν_5	2111	2119	84 S_1	1994	1985	58 S_1 + 28 S_4
	ν_6	1599	1598	86 S_2	1596	1597	85 S_2
	ν_7	1415	1415	18 S_{10} + 79 S_{11}	1415	1415	18 S_{10} + 78 S_{11}
	ν_8	1312	1309	72 S_{10}	1306	1309	71 S_{10}
	ν_9	1096	1097	16 S_3 + 76 S_{12}	1096	1094	15 S_3 + 78 S_{12}
	ν_{10}	874	875	57 S_3 + 24 S_{12}	865	866	56 S_3 + 22 S_{12}
	ν_{11}	625	632	111 S_{13}	543	542	25 S_8 + 59 S_9 + 19 S_{13}
	ν_{12}	539	539	21 S_8 + 65 S_9	490	483	97 S_{13}
	ν_{13}	217	215	94 S_8 + 19 S_9	205	206	91 S_8 + 18 S_9
a"	ν_{14}	974	974	17 S_{16} + 16 S_{17} + 89 S_{18}	974	974	17 S_{16} + 16 S_{17} + 89 S_{18}
	ν_{15}	927	927	84 S_{17}	926	927	84 S_{17}
	ν_{16}	677	677	74 S_{16}	676	676	76 S_{16}
	ν_{17}	618	619	102 S_{14}	490	489	107 S_{14}
	ν_{18}	304	305	98 S_{15}	290	290	89 S_{15}
	$\xi^a_{13,18}$	0.58	0.69		0.61	0.69	
	$\xi^b_{13,18}$	0.29	0.18		0.27	0.17	
	D_J	1.93	1.88		1.56	1.58	
	D_{JK}	-83.22	-80.76		-77.35	-74.90	
	D_K	2548.	2796.		2009.§	2892.	
	ID_c §	0.167	0.163		0.174	0.169	
	ID_{13} §	0.157	0.118		0.165	0.120	
	ID_{18} §	0.257	0.313		0.285	0.325	

* Potential energy distribution defined by: $PED_{ij} = 100 \cdot F_{ii} \cdot L^2_{ij}/\lambda_j$. Terms less than 15 have been omitted.

§ Not included in least squares fit.

In order to ensure convergence during the iterations some of the constants had to be constrained. We have constrained two pairs of stretch–bend interactions to be equal ($F_{D\beta} = F_{S\gamma}$ and $F_{D\omega} = F_{S\omega}$). Further, the stretch–stretch constants F_{SD} and F_{ST} were strongly correlated with the diagonal force constants and were fixed at reasonable values.

The final force field is presented in Table 7 while the observed and calculated values for the experimental data are listed in Table 8. As seen, the force constants are all of reasonable magnitudes and the agreement between the observed and the calculated data satisfactory except for the Coriolis coupling constants and the inertial defects for the $v_{13} = 1$ and $v_{18} = 1$ states. Calculations based upon a non-linear acetylene chain does not result in any improvement, and we believe that the discrepancies are due to large amplitude motions.

Acknowledgements—The authors are grateful to the Chemical Laboratory V, the H. C. Ørsted Institute, Copenhagen, for the use of their microwave spectrometer. Financial support from the Norwegian Research Council for Science and the Humanities is acknowledged.

REFERENCES

[1] K. W. F. KOHLRAUSCH, *Ramanspektren*, Akademische Verlagsgesellschaft, Leipzig (1943).
[2] N. SHEPPARD, *J. Chem. Phys.* **17**, 74 (1949).
[3] A. A. PETROV, V. A. KOLESOVA and J. I. PORFIRJEVA, *Zhur. Obshchei Khim.* **27**, 2081 (1957).
[4] F. BROGLI, E. HEILBRONNER, J. WIRZ, E. KLOSTER-JENSEN, R. G. BERGMAN, K. P. C. VOLLHARDT and A. J. ASHE III, *Helv. Chim. Acta* **58**, 2620 (1975).
[5] C. HIROSE, *Bull. Chem. Soc. Japan* **43**, 3695 (1970).
[6] H. W. MORGAN and J. H. GOLDSTEIN, *J. Chem. Phys.* **20**, 1981 (1952).
[7] G. A. SOBOLEV, A. M. SHCHERBAKOV and P. A. AKISHIN, *Optics Spectr.* **12**, 78 (1962).

[8] T. Fukuyama, K. Kuchitsu and Y. Morino, *Bull. Chem. Soc. Japan* **42,** 379 (1969).
[9] E. Tørneng, C. J. Nielsen, P. Klaeboe and H. Hopf, *J. Mol. Struct.* (in press).
[10] W. A. Seth-Paul, *J. Mol. Struct.* **3,** 403 (1969).
[11] G. O. Braathen, C. J. Nielsen, P. Klaeboe and H. Hopf (to be published).
[12] I. A. Mills, *8th European Congress on Molecular Spectroscopy, Copenhagen* 1965, Butterworths, London (1965).
[13] E. B. Wilson Jr., J. C. Decius and P. C. Cross, *Molecular Vibrations*. McGraw-Hill, London (1955).
[14] J. H. Schachtschneider, Vibrational Analysis of Polyatomic Molecules II, *Technical Report No. 210–61, Shell Develop. Company*, Emeryville, California (1961).
[15] R. Elst, W. Rogge and A. Oskam, *Recl. Trav. Chim. Pays-Bas*, **92,** 427 (1973).
[16] J. M. Freeman and T. Henshall, *J. Can. Chem.* **47,** 935 (1969).